Journal of Volcanology and Geothermal Research 328 (2016) 178–186

Contents lists available at ScienceDirect

Journal of Volcanology and Geothermal Research

journal homepage: www.elsevier.com/locate/jvolgeores

Influence of particle density on flow behavior and deposit architecture of concentrated pyroclastic density currents over a break in slope: Insights from laboratory experiments

Rodriguez-Sedano L.A. [a,*], Sarocchi D. [b,c], Sulpizio R. [d,e], Borselli L. [b], Campos G. [b], Moreno Chavez G. [b]

[a] Posgrado en Ciencias de la Tierra, Centro de Geociencias, Universidad Nacional Autónoma de México, Campus Juriquilla, Queretaro, Mexico
[b] Instituto de Geología/Fac. Ingeniería UASLP, Dr. M. Nava No 5, Zona Universitaria, 78240, San Luis Potosí, Mexico
[c] Department of Geosciences, Boise State University, 1910 University Drive, Boise, ID 83725-1535, United States
[d] Dipartimento di Scienze della Terra e Geoambientali, via Orabona 4, 70125, Bari, Italy
[e] IDPA-CNR, via M. Bianco 9, Milan, Italy

ARTICLE INFO

Article history:
Received 1 May 2016
Received in revised form 14 October 2016
Accepted 30 October 2016
Available online 3 November 2016

Keywords:
Laboratory experiments
Granular segregation
Concentrated pyroclastic density currents
Density contrast
Granular flows

ABSTRACT

Geological granular flows are highly complex, gravity-driven phenomena whose different behaviors depend on the mechanical properties, density and granulometric distributions of the constituent materials. Years of research have produced significant advances in understanding transport and deposition processes in granular flows. However, the role and effects of clast densities and density contrast in a granular flow are still not fully understood. In this paper we show the effect that pumice has on dry granular flows; specifically on flow velocity and longitudinal segregation of the deposits. Our work confirms, by experimental results, field observations on pumice/lithic segregation and longer pumice runout.

We report results of velocity decay and deposit architecture for a granular flow passing over a break in slope (from 38° to 4° inclination). The 30 experimental runs were carried out in a five-meter long laboratory flume equipped with a series of sensors that include laser gates and high-speed cameras (400 fps). We used two polydisperse mixtures of dacitic lithics and rhyolitic pumice in varying amounts, with Weibull and Gaussian particle size distributions.

The pumice/lithic ratio changes the flow response passing over a break in slope. This effect is particularly evident starting from 10% of pumice volume into the flow mixture, independently of its granulometric distribution. Runout relates to mass following a power law, with an exponent close 0.2.

The experiments confirm that pumice segregation affects polydispersed mixtures, similarly to what has been observed in real field deposits, where density decoupling produces lithic-enriched proximal areas and pumice-enriched distal areas. The results obtained prove that the presence of low-density materials in a dense granular flow has a strong influence on its behavior.

1. Introduction

Granular flows are among the most studied, yet not fully understood phenomena on Earth. Scientists have tried to explain their kinematics, segregation, rheology and many other aspects through a wide range of approaches and targets over the past decades (Pouliquen, 1999; Kueppers et al., 2012; Sulpizio et al., 2014, Lube et al., 2015).

Granular flows are a common phenomenon in everyday life, from industrial processes to large-scale granular flows in nature that can cause disasters such as landslides, debris flows and concentrate pyroclastic density currents (CPDCs).

Granular matter is defined as a set of particles that can be of different sizes, densities and shapes that can move independently and interact with each other (Kadanoff, 1999). Therefore, a granular flow could be defined as the movement and interaction of large quantities of particles of different sizes, shapes and densities that move in a liquid or gaseous medium.

One of the most interesting characteristics of polydisperse granular flows is particle segregation. When granular material is moving, particles are rapidly sorted as a function of their size, density and shape. Studies of segregation phenomena in granular flows are mostly focused on particle size segregation (Savage and Lun, 1988; Ottino and Khakhar, 2000), Particle segregation has been investigated using mathematical (Tripathi and Khakhar, 2011; Larcher and Jenkins, 2013; Larcher and Jenkins, 2015) and analogue modeling (Drahun and Bridgwater, 1983; Alonso et al., 1991; Hajra and Khakhar, 2005; Jain et al., 2005a, 2005b;

* Corresponding author.
E-mail address: lrodriguez2021@live.com.mx (L.A. Rodriguez-Sedano).

http://dx.doi.org/10.1016/j.jvolgeores.2016.10.017
0377-0273/

Larcher and Jenkins, 2013; Gray et al., 2015). All the above-mentioned literature deal with models based on simplified conditions (spherical particles, few particle size classes and artificial materials). Data on particle density segregation with natural material and using laboratory flumes is absent. Density segregation in volcanic granular flows has been investigated in debris flows (Dolan, 2004; Capra et al., 2004; Vallance, 2005), in CPDCs (Calder et al., 1999, 2000; Pittari et al., 2005), and using numerical simulations (Mitani et al., 2004). In CPDCs, low-density pumice segregation is an important factor that influences flow rheology, runout and the texture of the final deposits (Calder et al., 2000; Pittari et al., 2005). Both authors reported that pumice is segregated toward the upper and external regions of the flow, causing a significant rheological contrast with the lower, lithic-rich, denser zone. They also conclude that the upper and lighter pumice-rich zone can detach from the main flow as its lower, denser portion decelerates due to basal frictional forces, changes in slope or topographic barriers, and can run further ahead as a mobile derivate PDC. The vertical segregation of granular materials was also investigated by Cagnoli and Romano (2013), by means of laboratory experiments. They concluded that vertical segregation of materials can be generated by the imbalance of forces and the strong impulses due to collisions with the subsurface asperities.

Larcher and Jenkins (2015) formulate an improved kinetic theory, modeling the evolution in time and space of the relative concentration of bi-disperse systems of artificial spherical beads. Their model well describe the rates of segregation with time and distance as function of the flow depth, average particle size, flow inclination, restitution coefficient and the volume fraction of the species. The study of CPDC in natural settings has major limitations, due to their unpredictable behavior and hostile nature. Furthermore, the turbulent ash clouds that accompany moving CPDCs hinder direct observation of physical processes occurring in the basal part of the flow. Most of these difficulties can be overcome through laboratory experiments using granular flow simulators (experimental flumes; Iverson et al., 1992, Roche et al., 2004; Cagnoli and Romano, 2010; Dellino et al., 2007, 2010a, 2010b; Roche et al., 2010; Girolami et al., 2011; Lube et al., 2015).

The use of these facilities represents a unique opportunity for observing and measuring processes that can be scaled to real events (Iverson et al., 1992, Dellino et al., 2007, 2010a, 2010b, 2011, 2014; Sulpizio et al., 2009; Bartali et al., 2012, 2015; Dioguardi et al., 2013). Another advantage of laboratory experiments is the ability to control boundary conditions that can influence flow variables.

In this paper we present the results of laboratory experiments on polydisperse volcanic granular flows using natural particles of different densities. The flow kinematics, runout and deposit architecture are discussed and compared with three real cases of density-segregated CPDC deposits.

2. Materials and methods

All experiments were carried out using GRANFLOW-SIM (Fig. 1), a modular experimental flume designed and developed at the LAIMA (Image Analysis and Analogue Modelling Laboratory, for its Spanish acronym) at the Geology Institute of the Universidad Autónoma de San Luis Potosí, Mexico (Bartali et al., 2012, 2015). It consists of three main modules: i) a charge box, ii) a flume, and iii) an expansion box (Fig. 1). The charge box is made of waterproof PVC, has an electromagnetic lock at the bottom that can be opened remotely. It has a volume of 0.036 m^3, which is the volume for all mixtures used in this study. The charge box has a lateral window of tempered glass that allows the material inside to be viewed and can be placed at different heights (from 0.4 m to 2.7 m above the flume) according to the needs of the experiment. The flume is made of PVC plastic with a textile floor to increase friction, and is 4.9 m long and 0.3 m wide, with 0.25 m lateral walls of tempered glass. The flume has a straight channel that can be inclined at any angle from 0° to 45°. It is equipped with a series of sensors in the form of laser gates to measure the flow front velocity. The laser beam sensors are positioned at 1.5 cm from the flume bottom. There are nine gates along the flume (Fig. 1). These gates consist of a laser source and a photodiode receptor, and are placed outside the glass walls. When the granular flow front crosses the laser gate, the light beam is interrupted and the time automatically recorded. This allows calculating velocity of the flow front along the flume. At each laser barrier the velocity was calculated using the central difference rule, which was adopted in order to reduce the approximation error in velocity calculation.

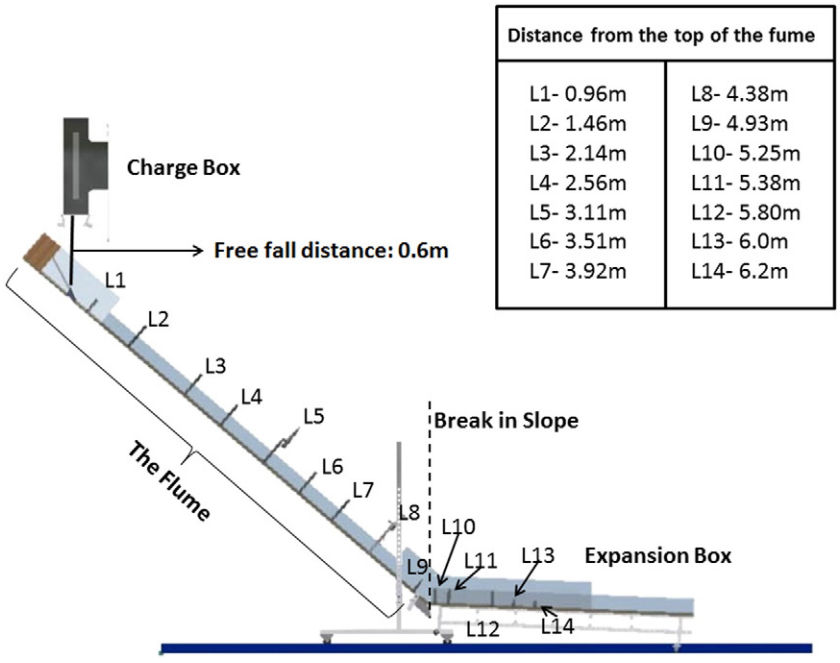

Fig. 1. Diagram of GRANFLOW-SIM experimental flume. L1–L14 indicate positions of laser gates. The flume can be inclined from 0° to 45°. The sedimentation module can be inclined from 0° to 25°.

In this study we used only the values of the lasers 9 and 10 (the lasers before and after the break in slope) in order to get the velocity changes after a break in slope. The expansion box is 2.4 m long and 1.2 m wide, with 0.25 m glass sidewalls. This module can be inclined between 5° and 25°, and is equipped with five laser gates (Fig. 1). For our experiments we used two glass walls (0.25 m high and 1.5 m long) that channelize the flows in the expansion box. These walls are used to simulate the behavior of CPDCs in a ravine with vertical walls.

Three high-speed camcorders (Nikon 1S1 and J1, 400 fps) complete the recording equipment. The camcorders can be placed at any position along the flume and the expansion box.

Pyroclastic mixtures (lithics and pumices) with two different grain size distributions (Gaussian and Weibull) were used for the experiments (Fig. 2). The use of Gauss and Weibull distributions is justified because they are classic grain size distribution common in many natural, transported sediments (Wohletz et al., 1989, Wohletz et al., 1995). The used grain size classes are $-3\ \phi$ (8–16 mm), $-2\ \phi$ (4–8 mm), $-1\ \phi$ (2–4 mm), $0\ \phi$ (1–2 mm) and $1\ \phi$ (0.5–1 mm) ($\phi = -\log_2 d$, where d is the particle diameter). Five different pumice–lithic volume ratios were created for each of the two grain size distributions. Fig. 2 shows Gaussian distributions with the different pumice–lithic proportions, where GP0 (GP stands for Gaussian Pumice 0%) and GP100 (Gaussian Pumice 100%) represent mixtures made up exclusively of lithics and pumice, respectively. The Gaussian distribution is defined by mean $-1.0\ \phi$ (2 mm) and standard deviation $1.0\ \phi$ (0.5 mm). The Weibull distribution is defined as a three-parameter Weibull distribution type by the parameters scale (alpha) = 2.26, shape (beta) = 2.18, and shift (lambda) = $-4.3\ \phi$, which corresponds to mean $-2.3\ \phi$ (4.9 mm), standard deviation 0.97 ϕ (0.51 mm) and skewness $+0.51\ \phi$.

For this study all mixtures were prepared using constant volume of 0.036 m^3. We produced several mixtures with variable mass and densities (Table 1), spanning from 1440 kg/m^3 for the pure lithic Gaussian distribution (GP0) to 690 kg/m^3 for the pure pumice Gaussian distribution (GP100). And from 1360 kg/m^3 for pure Weibull distribution (WP0), to 600 kg/m^3 for pure pumice Weibull distribution (WP100). Velocities of all the experiments are listed in the appendix (Table A1).

The volcanic material consists of low-density (760 kg/m^3) rhyolitic pumice and dense (2700 kg/m^3) dacitic lithics.

The angle of repose was measured using the cylinder method. A 1×10^{-3} m^3 sample was placed inside a cylinder (20 cm high and 10.5 cm in diameter). A wooden plate covered by the rubber floor (the same as the flume) was placed at the base of the cylinder. The slow lifting of the cylinder produces a stack of granular material whose slope corresponds to the angle of repose (Fig. A1).

For each experiment the charge box was completely filled with the mixture, and the granular material was released into the flume after a free fall of 0.6 m. The falling material impacts the flume on a small ramp having an inclination of 20°, in order to smooth the transition between free falling and flowing along the channel. As the granular flow developed, sensors recorded the passage of the material until it came to a complete rest. Two data cards (Texas Instruments® and MDA® which record at 15,000 samples per second per channel) were used for data capture on a laptop.

Each experiment consists of three runs with the same initial and boundary conditions (Table 1). A total of 30 runs corresponding to 10 different experiments were carried out with the same flume configuration (channel slope 38°, expansion box slope 4°). The deposit formed after each run was photographed at high resolution for image analysis.

In order to measure runout we first individuated the flow front border (Fig. 3). We consider the flow front as the distal part of the deposit where clasts are still in touch to each other (Fig. 3), forming a compact body of grains. Measures were taken at this point.

In order to better compare the results of different runs, the experimental data (velocity, mass and runout) were normalized against the maximum-recorded value for each parameter. Velocity at laser 9 was normalized against the maximum velocity registered for all experiments at this point. For runout, data were normalized against the maximum runout measured, while the mass was normalized versus the maximum mass. Once all values were normalized, the mean value and standard deviation of each experiment (3 runs) was calculated.

Image analysis of two experimental deposits (GP50 and WP50 runs) enabled the longitudinal segregation of pumice to be studied. Lateral photographs of the deposit were taken and a panoramic image of the whole micro-deposit was constructed. The resulting images were divided longitudinally into equal areas (taking the change in slope as the starting point). A count of the number of pumice and lithic particles was made for each area using the Image Pro Plus Software (Media Cybernetics Inc.). By using this semi-manual technique, it is possible to quantify the lateral segregation of pumice and lithic particles along the deposits. In both case-study data shown trends, although in one case data are scattered. For this reason, a quantile regression method (Buchinsky, 1998; Koenker and Basset, 1978; Lee and Tanaka, 1999; Yu et al., 2003), as implemented by Borselli et al. (2012), is used to analyze the produced dataset. The quantile regression technique is useful in these cases because it is more robust against local outliers influence and can provide more robust measures of central tendency and statistical dispersion. We use three relevant quantiles in a distribution: q(0.5) is the median and can be used to represent the main trend function of the data, q(0.25) and q(0.75) represent the values farthest away from

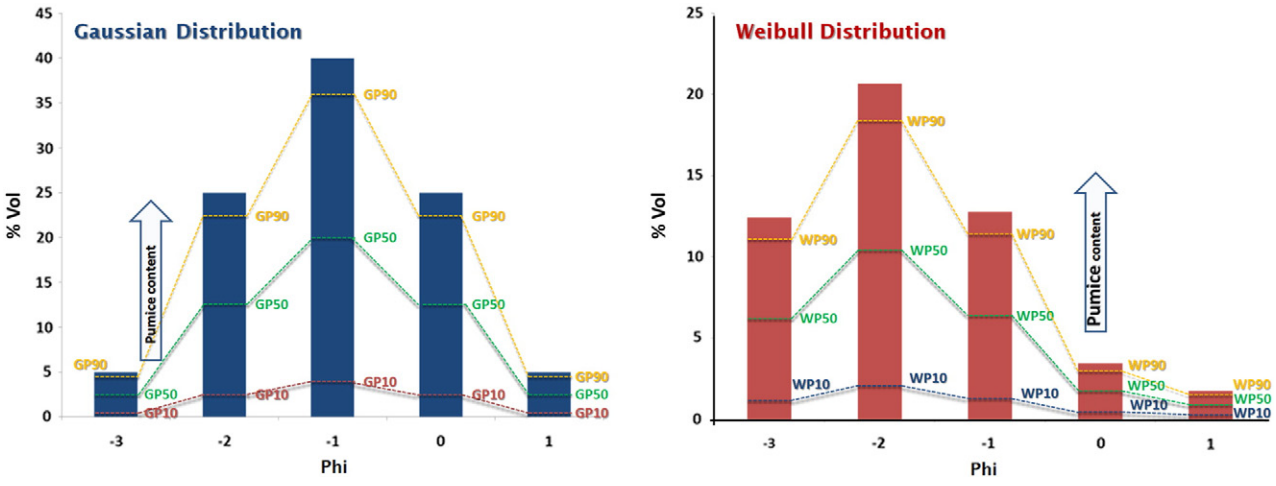

Fig. 2. Granulometric distributions and pumice proportions used for these experiments.

Table 1
Experimental setup and mixture characterization values.

Label	P (% in vol.)	RO mean (cm)	RO stdev (cm)	RO cv (%)	RA (°)	FI (°)	EBA (°)	Rep. num.	MTM (kg)	MNTM (kg)	MV (dm^3)	MAD (gr/cm^3)	MPM (kg)	RO nor.	RO nor. stdev
GP0	0% pum	151.67	2.887	1.903	29°	38°	4°	3	52	1.000	36.0	1.44	0.000	0.978	0.019
GP10	10% pum	147.67	2.517	1.704	28°	38°	4°	3	44.25	0.851	36.0	1.23	2.490	0.953	0.016
GP50	50% pum	139.33	4.041	2.901	32°	38°	4°	3	34.8	0.669	36.0	0.97	12.450	0.899	0.026
GP90	90% pum	135.00	2.000	1.481	30°	38°	4°	3	31.05	0.597	36.0	0.86	22.410	0.871	0.013
GP100	100% pum	123.00	2.646	2.151	28°	38°	4°	3	24.9	0.479	36.0	0.69	24.900	0.794	0.017
WP0	0% pum	146.67	2.887	1.968	31°	38°	4°	3	48.9	0.940	36.0	1.36	0.000	0.946	0.019
WP10	10% pum	143.33	2.887	2.014	30°	38°	4°	3	42.65	0.820	36.0	1.18	2.190	0.925	0.019
WP50	50% pum	135.00	5.000	3.704	28°	38°	4°	3	33.7	0.648	36.0	0.94	10.950	0.871	0.032
WP90	90% pum	135.00	2.000	1.481	30°	38°	4°	3	24.65	0.474	36.0	0.68	19.710	0.871	0.013
WP100	100% pum	121.67	2.887	2.373	31°	38°	4°	3	21.9	0.421	36.0	0.61	21.900	0.785	0.019

Label	MTM (kg)
Pumice proportion	Mixture total mass (kg)
Runout (mean) (cm)	Mixture normalized total mass
Runout standard deviation (cm)	Mixture volume (dm^3)
Runout variation coefficient (%)	Mixture apparent density (gr/cm^3)
Repose angle	Mixture pumice mass (Kg)
Flume inclination	Mixture pumice fraction by volume
Expansion box angle	Mixture pumice fraction by mass
Number of repetitions	Normalized runout
	Standard dev. runout normalized

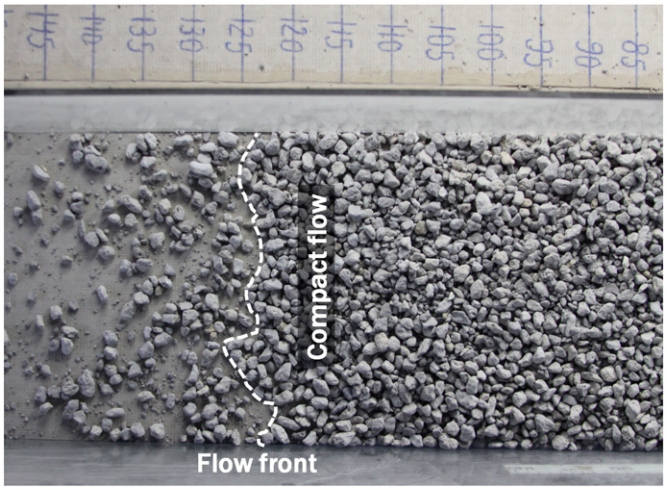

Fig. 3. Photograph that illustrates the compact flow front. We used the compact flow front to measure the runout of the flows.

the median and can be used to define the boundaries in which the values are most reliable. In our case we carry out the quantile regression using an exponential function as Eq. ((1), and using Microsoft® Excel Spreadsheet Office 2013 Solver (Fylstra et al., 1998; Nenov and Fylstra, 2003):

$$P(d) = be^{da} \tag{1}$$

where P is % pumice; d is the normalized distance from the break in slope using the maximum recorded runout (GP0 mixture), b and a are quantile regression coefficients. For more information about quantile function the reader is addressed to Appendix A2.

3. Results

3.1. Changes in velocities and runout induced by break in slope

Flow velocity and runout were measured for the two granulometric distributions (Weibull and Gaussian) with five different pumice/lithic proportions (Table 1). The results presented here report flow velocities recorded just before and after the break in slope. At laser 9 it is possible to observe the maximum velocities of any type of mixture, while on laser 10 it is possible to see how each mixture responds to a topographic change (slope change from 38° to 4°).

Three main groups with similar behavior can be identified. The first is pumice-rich and comprises WP100 and GP100 (Group A), the second WP90, WP50, GP90 and GP50 (Group B), and the third group is lithic-rich and consists of the WP10, WP0, GP10 and GP0 distributions (Group C; Fig. 4).

Group A has an average mass of 23.3 ± 1.5 kg. Group B is mostly made of pumice-rich to equal lithic/pumice distributions, with an average mass of 31 ± 1.51 kg. Group C has an average mass of 46.8 ± 1.5 kg.

Prior to the change in slope, all the mixtures move at comparable average velocities, with the only exception of GP0 (Fig. 4a, c). The velocity is not affected by the mass, with the only exception of GP0. After the break in slope the average velocities roughly separate between Gaussian and Weibull distributions, although large overlapping of values is observable and the suggested difference has poor statistical meaning (Fig. 4b, d). Also in this case the mass does not seem to significantly influence the velocity.

In Group A WP100 shows an increase in average velocity after the change in slope. This velocity is in the same range as the fastest mixtures (of group C) before the change in slope, and is one of the three fastest velocities recorded of all groups. In contrast GP100 undergoes a strong decrease in velocity, making it one of the slowest mixtures after the

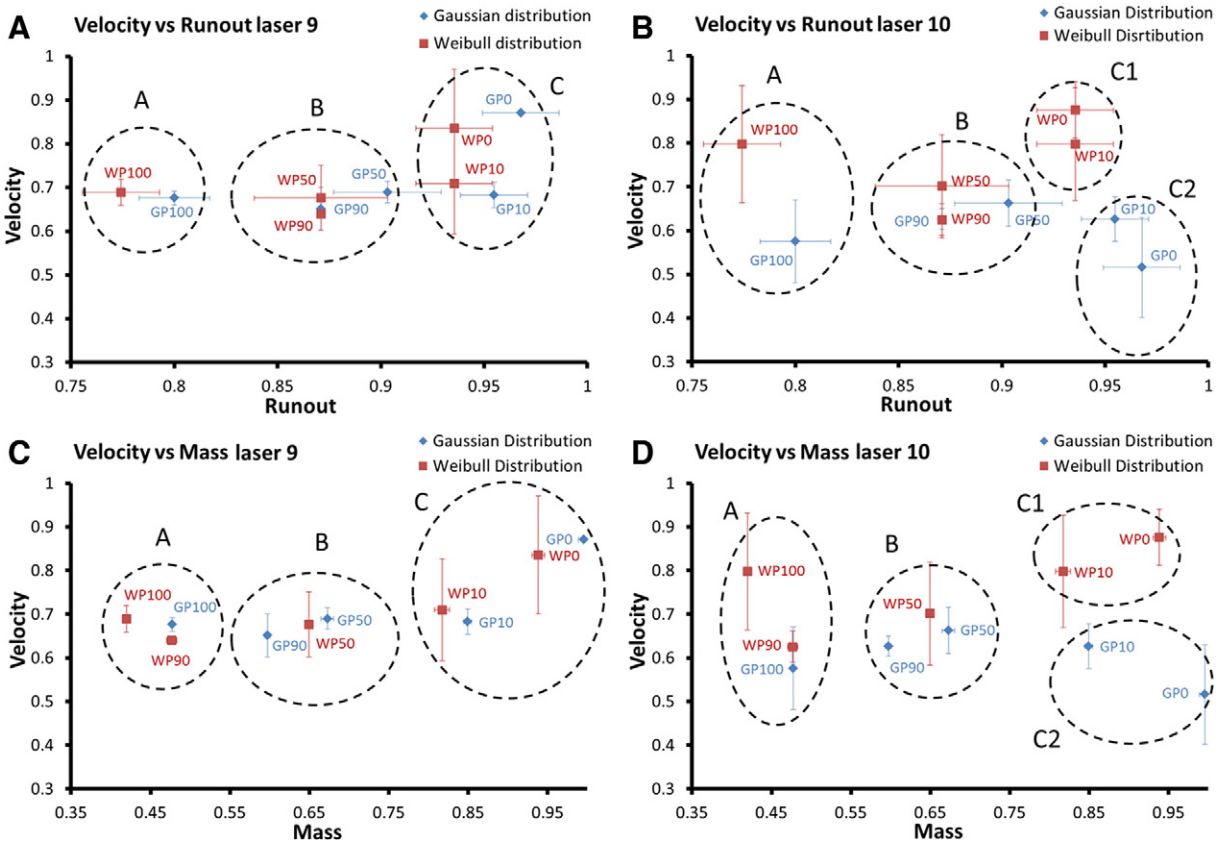

Fig. 4. Normalized velocity before (laser 9) and after (laser 10) the break in slope compared to normalized runout (3a and b) and mass (3c and d). It is possible to observe the different behavior of any mixture to the change in slope, as well as the three main groups according to the runout.

change in slope (Fig. 4). Group B does not show appreciable change in velocity before and after the break in slope (Fig. 4). Group C mixtures are some of the fastest mixtures before the change in slope (WP0 and GP0; Fig. 3a). After the change in slope, WP and GP mixtures preserve their velocity but in different ways, forming two sub-groups (C1 and C2; Fig. 4b and d). GP mixtures presented a loss in average velocity, especially GP0, which in this case had the lowest velocity of all. The C2 sub-group is made up of only GP mixtures. WP mixtures fall into the C1 subgroup. GP10 and W10 show decrease in their average velocities after the change in slope.

Analyzing the runouts vs. mass, Group A mixtures (the lightest in mass) have the shortest runouts of all (Fig. 5b). GP0 had the maximum velocity, the longest runout and the highest mass of all the mixtures (Fig. 5b). The normalized runout vs. normalized mass diagram indicates similar power law relationship for both Gaussian and Weibull distributions (Fig. 5a, b). The regression functions for Gaussian and Weibull distribution are quite similar (Fig. 5b), and, in average, can be expressed as:

$$N_r = 0.973 NTM^{0.2103} \quad (2)$$

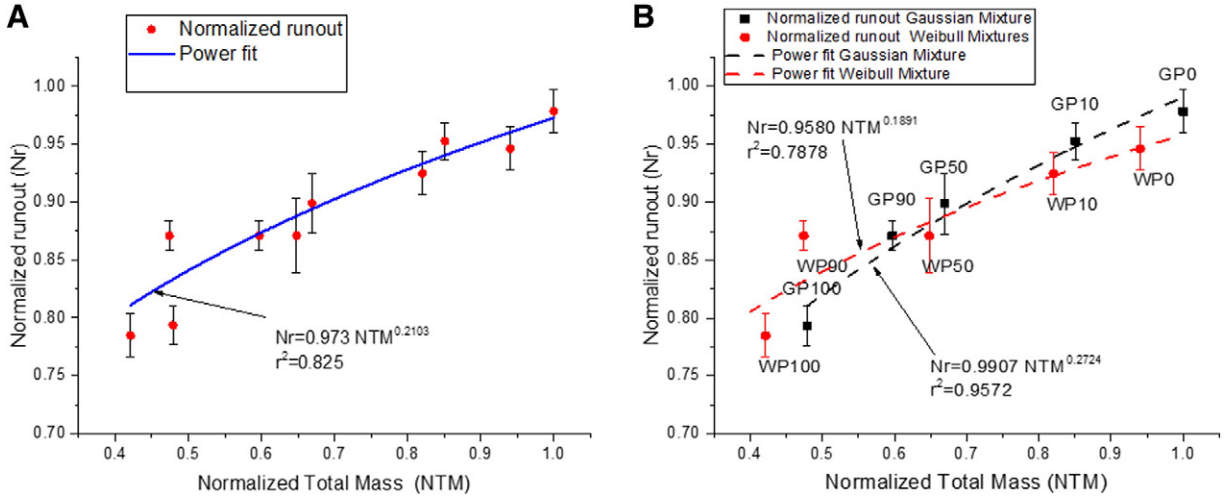

Fig. 5. Normalized runout vs. normalized mass and vs. pumice fraction by mass in the mixtures: a) Normalized rounout vs. normalized mass, global data; b) Normalized rounout vs. normalized mass , with separate mixtures type groups.

3.2. Longitudinal pumice distribution along the deposits

In order to study the segregation behavior of clasts in a mixture with different densities, a quantitative study was made of the GP50 and WP50 deposits.

A panoramic image of the experimental deposit was divided into sectors of equal area. In order to obtain the longitudinal variation of the pumice/lithic ratio, the panoramic image of GP50 (blue; Fig. 6) was divided into 52 sectors each 2.6 cm wide. Pumice and andesite particles were counted (a total of 5636 particles in the image in Fig. 6).

Pumice fragments are preferentially concentrated in the upper part of the deposit. The deposit shows a pumice concentration ranging between 50% and 60% starting from the break in slope, but after 70 cm (0.5 normalized distance), which corresponds approximately to the center of mass of the deposit, pumice content starts to gradually increase and lithic content to decrease. At 110 cm (0.7 normalized distance), it starts to show sectors formed exclusively by pumice.

The same experiment was performed using the WP50 mixture (Fig. 6, red). This deposit was split into 47 sectors 2.8 cm wide and 4725 particles were counted. In this case the longitudinal distribution of pumice was more disperse, but showed the same trend. At 70 cm from the break (0.5 normalized distance) the percentage of pumice in the deposit ranged from 50% to 90% and it was not until after 110 cm (0.7 normalized distance) that the percentage of pumice within the deposit reached 100%.

4. Discussion

Granular mixtures with different granulometry and pumice contents, having the same volume and flowing at the same experimental conditions, show different behaviors. Distinct groups of runouts were identified, which did not depend on the initial velocity. The main factor that affects such behavior is the mass (Figs. 4 and 5). This is because the normalized velocities overlap, irrespective of mixture and grain size distributions (Fig. 4).

4.1. Influence of grain size on velocity and runout

Before the break in slope, both Weibull and Gaussian distributions do not show any significant difference in velocity. After the break in slope, the Weibull (coarse grained) distributions show, on average, slightly higher values of velocity than the Gaussian (finer grained) distributions, although the difference is not statistically representative. This may be explained in terms of the inertial properties of the two

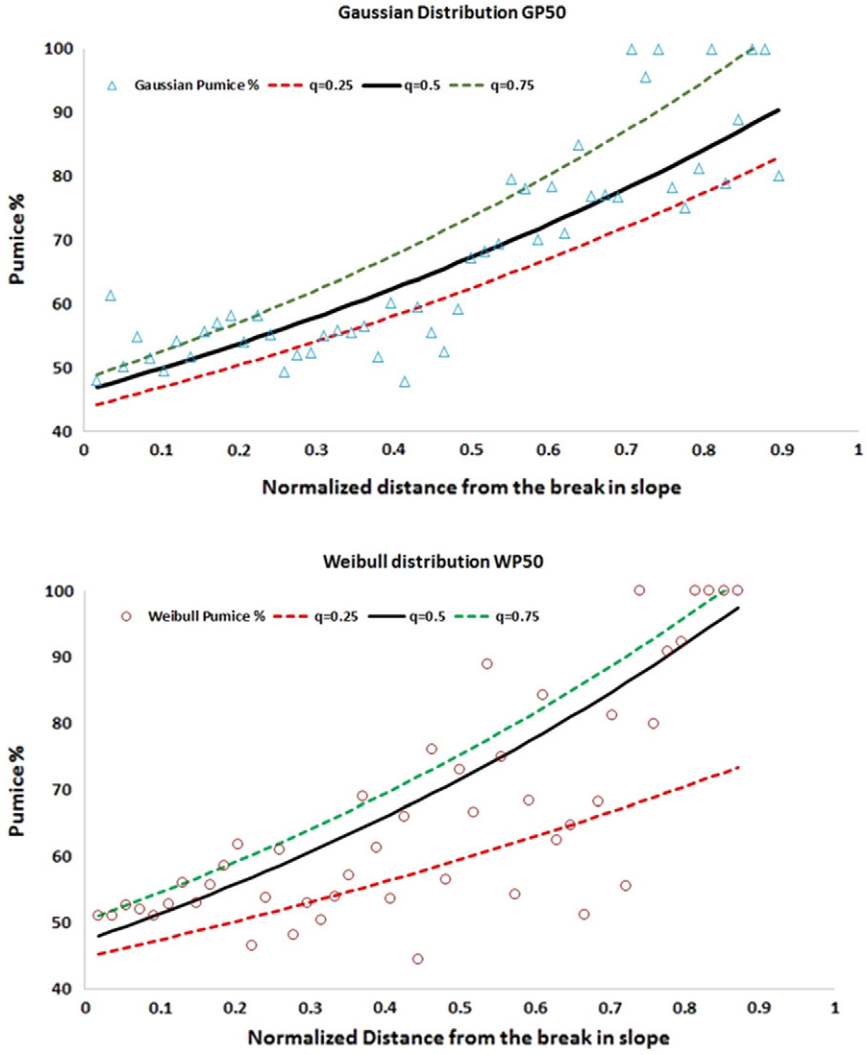

Fig. 6. Longitudinal variation in pumice content (expressed as percentage) from the break in slope to the maximum runout of the GP50 and WP50 mixtures. Distance was normalized against the maximum runout of all mixtures, which was GP0. Black line represents q0.5 of all data.

distributions. Finer particles have lower inertia than coarser particles (coarse particles are more agitated) and this contributes to slowing down the velocity after the break in slope, which is the first physical perturbation in the rectilinear trajectory. Mixtures with a similar fraction of lithics and pumice (50% lithics, 50% pumice) in both the Weibull and Gaussian distributions do not show any significant change in velocity, while the other Weibull mixtures show a slight increase in average velocity and the Gaussian mixtures show an average reduction of velocity after the break in slope (Fig. 4). This is probably due to the bouncing effect of large clasts at the break in slope, with elastic rebound at the base that accelerates the coarsest clasts. This is particularly evident in the case of Weibull distributions, which have a larger amount of coarser clasts. On average, runout is greater for finer mixtures, but it is worth noting that error bars overlap in all cases (Fig. 5). Longer runouts for finer grained flows were suggested by Cagnoli and Romano (2012) and Cagnoli and Piersanti (2015), due to the greater energy consumption of shacked coarse particles with respect to the finer ones. Our experiments results are not in contrast with this suggestion, although it is not statistically relevant for the grain size distribution we used. Finally particle agitation dissipates energy because it requires speed components in random directions. That could be the reason why Gaussian mixtures (finer grain size) reach a little bit longer runouts than Weibull ones (coarser grain sizes).

4.2. Influence of mass (pumice/lithic ratio) on velocity and runout

All the mixtures move at same velocity (within the error bar) before the break in slope (Fig. 4a, c), irrespective of their mass. Inspection of Fig. 5 shows how the normalized runout has power law dependence on the normalized mass. The regression functions for Gaussian and Weibull distribution are quite similar, and can be expressed with exponent close to 0.2 (Eq. (2)). It means that up to 0.5–0.6 of normalized mass value (~25–32 kg), a slight increase in mass of the mixture produces a significant larger runout. This effect is reduced for values of normalized mass greater than 0.7 (~35 kg). If we consider the runout as the balance between inertial/frictional forces, it seems that pumice clasts increase friction and lithic fragments increase inertia. This is probably due to the different elastic properties of the two components (pumice and lithics) of the mixtures, which dissipate kinetic energy in different ways even at similar (within 10%) mass of the mixtures.

The normalized runout drop down with increase of pumice fraction by mass (with constant volume of the mixture) following a linear law as indicated in Fig. 5a and b, and this is related to the progressive decrease of mass due to increase of total pumice fraction. All the experiment was planned in order to evaluate the flow behavior with different mass but with constant flow volume.

It is important to note that Gaussian mixtures always show longer runouts than the correspondent Weibull mixtures. This is related to the masses of the mixtures; Gaussian mixtures are heavier than Weibull, although they have the same volume and granulometric distribution. The greater the mass the greater the inertia and therefore this will be reflected in the runout results.

4.3. Pumice–lithic segregation with distance

The experiments with 50% pumice, in which the most important velocity conservation was observed, were also used to study the segregation effects between pumice and lithics inside the final deposits at rest. Fig. 6 shows the percentage of pumice present in the resulting deposits at different relative distances from the break in slope.

Two types of segregation were observed acting at the same time in our experiments: segregation by size and density. In general the segregation process appears to be more efficient for the Gaussian mixtures (finer grain sizes). Reverse grading was observed in both GP50 and WP50 mixtures. The coarsest clasts of both materials were concentrated at the top of the deposits, and in the case of Weibull mixture, also in the distal part. Concerning the segregation for density, this is more evident in the Gaussian mixture and longitudinally along the deposits. Data concerning pumice distributions in the deposits are more scattered in the case of the Weibul mixture where the coarse clasts are more abundant. This observation suggests that in coarsest mixtures the segregation process by size may be predominant.

The segregation process observed in our experiments supports observations on natural cases of PDCs where segregation of pumiceous materials has been observed (Calder et al., 1999; Calder et al., 2000; Pittari et al., 2005), as well decoupling of the less dense portion, which is usually concentrated in the upper portions of the flow. This separation generally leads to a secondary flow consisting mostly of pumice, which runs longer and affects a more extensive area. The denser lithic portion is deposited on more proximal areas, resulting in deposits with greater pumice content in distal areas. Similar behavior was observed in our laboratory experiments. Fig. 6 shows that the distal portion of the studied deposit has higher pumice content than the proximal areas.

At approximately 70 cm (0.5 normalized distance) from the change in slope, the pumice content starts to increase and concentrate toward the top, forming two layers with different properties. According to Calder et al. (2000), the interface between the layers becomes the zone of greatest shear due to the very different properties of pumices and lithics (density, restitution coefficient, friction coefficient, particle shape etc.) Buesch (1992) suggested that decoupling might occur due to inefficient transfer of momentum between the upper pumice layer and the lower and denser lithic layer. According to our data and observing how the velocity changes after the change in slope for different mixtures (i.e. a mixture made of pumice and one of lithics), it is understandable that reactions of flows to a change in slope are extremely different, so an efficient energy transfer between materials (lithics and pumice) could be not fully achieved, and decoupling (independently of the scale) would occur.

5. Conclusions

The experiments described here reveal important information about granular flows constituted of mixtures with materials of different density and elastic properties.

According to these results, the pumice/lithic ratio in a polydisperse natural granular flow influences the flow runout and, even roughly, the velocity after the break in slope. Polydisperse monolithologic mixtures composed of 100% pumice or 100% dense lithics have a more evident response to changes in slope, gaining or losing velocity. Flow velocity is directly related to inertial forces and elastic properties of the materials and how they respond to a break in slope. Granulometry has an important role because the bouncing effect of large clasts at the break in slope is very different in Weibull mixtures (coarse) and Gaussian mixtures (finer).

Runout relates to mass, following a power law with 0.2 exponent (Eq. (2)). Mixtures fully composed of lithics have far longer runouts than fully pumiceous mixtures of the same granulometry. This is because at equal volumes Gaussian mixtures are heavier than Weibull mixtures (due to granulometric distributions), which means Gaussians are denser and therefore have greater inertia than Weibull mixtures.

Deposits of CPDC with mixtures of pumice and lithic clasts in the Montserrat, Tenerife and Lascar volcanoes show a clear density segregation/separation, which ends with deposits made up mostly of lithic fragments in proximal areas and mostly pumiceous in distal areas. Experiments carried out in our flume reproduced similar behavior and produced deposits that show very similar characteristics. Our

experiments show enriched pumice content in the distal parts of the deposits, in analogy with what is observed in nature. The presence of a less effective pumice segregation in Weibull mixture deposits suggests that in coarse mixture segregation for size is probably more efficient than the segregation for density contrast.

The results of our study show that the pumice/lithic ratio in pyroclastic density currents affects their behavior. This effect is particularly evident for pumice content greater than 10% vol. Taking into account the density factor in programs that simulate PDCs can help in calculating more realistic hazardous areas.

Acknowledgments

We wish to thank Oscar Segura Cisneros, Sergio Gonzalez Bautista, Ludving Rojano and Luis Felipe Rodriguez Quibrera for their help during the experimental work. We are also grateful to Margaret Schroeder Urrutia for refining the English version of the paper.

This work was partially supported by Ciencia Básica CONACyT projects (SEP-83301), and CONACYT - Ciencia Básica-2012-01-184060, PROMEP UASLP-PTC-241. Luis Angel Rodriguez Sedano acknowledges CONACYT for PhD grant (No. 245245).

Appendix A1

The angle of repose was measured using the cylinder method (Fig. A1). The material flows from the base when the cylinder rises slowly. The static internal friction angle corresponds to the slope of the pile of granular material.

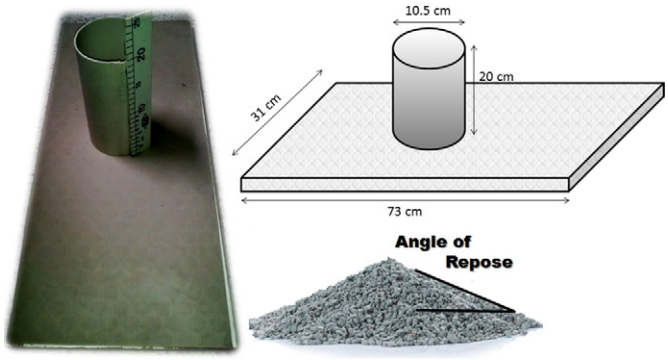

Fig. A1. Instrumentation and methodology used to obtain the repose angle in these experiments.

Table A1
Velocity in all lasers (m/s).

Laser	L1	L2	L3	L4	L5	L6	L7	L8	L9	L10	L11	L12	L13	L14
Dist. (m)	0.96	1.46	2.14	2.56	3.11	3.51	3.92	4.38	4.93	5.25	5.38	5.80	6.00	6.20
GP0	2.43	3.33	3.94	3.62	4.84	4.80	4.03	5.55	6.65	4.60	3.10	3.18	2.10	1.70
GP10	2.42	3.35	3.80	3.62	4.67	4.42	4.35	4.58	5.21	5.58	3.96	3.42	2.17	1.29
GP50	2.40	3.22	3.82	3.68	4.51	4.37	4.39	4.94	5.27	5.90	3.62	2.79	2.22	1.81
GP90	2.40	3.17	3.78	3.62	4.33	4.74	4.12	4.94	4.97	5.58	3.52	3.18	2.24	1.37
GP100	2.39	3.15	3.72	3.32	4.59	4.28	4.21	5.16	5.16	5.13	2.76	2.95	2.10	0.75
WP0	2.40	3.08	3.85	3.49	5.32	4.37	3.59	4.99	6.38	7.80	3.96	2.95	1.86	1.34
WP10	2.40	3.09	3.89	3.59	4.37	4.97	3.73	4.94	5.42	7.11	3.63	3.02	1.92	1.10
WP50	2.37	2.96	3.58	3.38	4.30	5.53	3.77	5.05	5.16	6.25	4.23	2.55	2.17	1.59
WP90	2.37	3.08	3.78	3.22	4.67	4.37	3.88	5.04	4.89	5.57	4.89	3.45	1.38	1.59
WP100	2.39	3.08	3.64	3.38	4.30	4.15	3.73	4.32	5.26	7.11	3.63	2.55	1.67	0.41

Appendix A2

According to Koenker and Basset (1978) the optimal quantile regression function $q_p\ (x)$ may be obtained by minimizing the following generalised objective function $f(obj)$:

$$f(obj) = \min_{\beta}\Big[\sum_{i\in\{i:y_i\geq f_i(\beta^t,x_i)\}} p|y_i - f_i(\beta^t,x_i)| \;+\; \sum_{i\in\{i:y_i<f_i(\beta^t,x_i)\}} (1-p)|y_i - f_i(\beta^t,x_i)|\Big] \tag{2}$$

where:
i is the index that identifies element i of the data set;
x_i, y_i are the coordinates of the ith element of the data set;
p is the chosen regression quantile (e.g.: 0.1, 0.5, 0.75 …);
β^t is a vector that contains the values of the coefficients defining the quantile function to be optimized (i.e., coefficients a and b, to be found during the optimization process);
$f_i(\beta^t,x_i)$ is the regression quantile function as defined by $\beta^t\beta^t$ and the position x_i.
The objective function (Eq. ((2)) was implemented in the Solver for a set of quantile values (0.25, 0.5, 0.75) for Weibull and Gaussian datasets.

References

Alonso, M., Satoh, M., Miyanami, K., 1991. Optimum combination of size ratio, density ratio and concentration to minimize free surface segregation. Powder Technol. 68, 145–152.
Bartali, R., Sarocchi, D., Nahmad-Molinari, Y., Rodríguez-Sedano, L.A., 2012. Estudio de flujos granulares de tipo geológico por medio del simulador multisensor GRANFLOW-SIM. Bol. Soc. Geol. Mex. 64, 265–275.

Bartali, R., Sarocchi, D., Nahmad-Molinari, Y., 2015. Stick–slip motion and high speed ejecta in granular avalanches detected through a multi-sensors flume. Eng. Geol. 195, 248–257.
Borselli, L., Torri, D., Poesen, J., Laquinta, P., 2012. A robust algorithm for estimating soil erodibility in different climates. Catena 97, 85–94.
Buchinsky, M., 1998. Recent advances in quantile regression models. J. Hum. Resour. 33, 88–126.
Buesch, D.C., 1992. Incorporation and redistribution of locally derived lithic fragments within a pyroclastic flow. Geol. Soc. Am. Bull. 104, 1193–1207.
Cagnoli, B., Piersanti, A., 2015. Grain size and flow volume effects on granular flow mobility in numerical simulations: 3-D discrete element modeling of flows of angular rock fragments. J. Geophys. Res. 120:2350–2366. http://dx.doi.org/10.1002/2014JB011729.
Cagnoli, B., Romano, G.P., 2010. Effect of grain size on mobility of dry granular flows of angular rock fragments: an experimental determination. J. Volcanol. Geotherm. Res. 193, 18–24.
Cagnoli, B., Romano, G.P., 2012. Effects of flow volume and grain size on mobility of dry granular flows of angular rock fragments: a functional relationship of scaling parameters. J. Geophys. Res. 117, B02207. http://dx.doi.org/10.1029/2011JB008926.
Cagnoli, B., Romano, G.P., 2013. Vertical segregations in flows of angular rock fragments: Experimental simulations of the agitation gradient within dense geophysical flows. J. Volcanol. Geotherm. Res. 265, 52–59.
Calder, E.S., Cole, P.D., Dade, W.B., Druitt, T.H., Hoblitt, R.P., Huppert, H.E., Richie, L., Sparks, R.S.J., Young, S.R., 1999. Mobility of pyroclastic flows and surges at the Soufriere Hills Volcano, Montserrat. Geophys. Res. Lett. 26, 537–540.
Calder, E.S., Sparks, R.S.J., Gardeweg, M.C., 2000. Erosion, transport and segregation of pumice and lithic clasts in pyroclastic flows inferred from ignimbrite at Lascar Volcano, Chile. J. Volcanol. Geotherm. Res. 104, 201–235.
Capra, L., Poblete, M.A., Alvarado, R., 2004. The 1997 and 2001 lahars at Popocatépetl volcano (central Mexico). Textural and sedimentological evidences to constrain their origin and hazard. J. Volcanol. Geotherm. Res. 131, 351–396.
Dellino, P., Zimanowski, B., Buttner, R., La Volpe, L., Mele, D., Sulpizio, R., 2007. Large-scale experiments on the mechanics of pyroclastic flow: design, engineering, and first results. J. Geophys. Res. 112, B04202. http://dx.doi.org/10.1029/2006JB004313.
Dellino, P., Buttner, R., Dioguardi, F., Doronzo, D.M., La Volpe, L., Mele, D., Sonder, I., Sulpizio, R., Zimanowski, B., 2010a. Experimental evidence links volcanic particle characteristics to pyroclastic flow hazard. Earth Planet. Sci. Lett. 295, 314–320.
Dellino, P., Dioguardi, F., Zimanowski, B., Buttner, R., Mele, D., La Volpe, L., Sulpizio, R., Doronzo, D.M., Sonder, I., Bonasia, R., Calvari, S., Marotta, E., 2010b. Conduit flow experiments help constraining the regime of explosive eruptions. J. Geophys. Res. 115, B04204. http://dx.doi.org/10.1029/2009JB006781.
Dellino, P., De Astis, G., La Volpe, L., Mele, D., Sulpizio, R., 2011. Quantitative hazard assessment of phreatomagmatic eruptions at Vulcano (Aeolian Islands, Southern Italy) as obtained by combining stratigraphy, event statistics and physical modelling. J. Volcanol. Geotherm. Res. 201, 364–384.
Dellino, P., Dioguardi, F., Mele, D., D'addabbo, M., Zimanowski, B., Büttner, R., Doronzo, D.M., Sonder, I., Sulpizio, R., Dürig, T., La Volpe, L., 2014. Volcanic jets, plumes and collapsing fountains: evidence from large-scale experiments, with particular emphasis on the entrainment rate. Bull. Volcanol. 76, 834–852.
Dioguardi, F., Dellino, P., De Lorenzo, S., 2013. Integration of large-scale experiments and numerical simulations for the calibration of friction laws in volcanic conduit flows. J. Volcanol. Geotherm. Res. 250, 75–90.
Dolan, M.T., 2004. Observatins of Lahars Along the Sacobia-Bamban River Systems, Mount Pinatubo, Philippines. ((48 pp.). MS thesis). Michigan Technologica l University, Houghton, Michigan .
Drahun, J.A., Bridgwater, J., 1983. The mechanisms of free surface segregation. Powder Technol. 36, 39–53.
Fylstra, D., Lasdon, L., Watson, J., Waren, A., 1998. Design and use of the Microsoft Excel Solver. Interfaces 28 (5), 29–55.
Girolami, L., Roche, O., Druitt, T.H., Corpetti, T., 2011. Particle velocity fields and depositional processes in laboratory ash flows, with implications for the sedimentation of dense pyroclastic flows. Bull. Volcanol. 72, 747–759.
Gray, J.M.N.T., Gajjar, P., Kokelaar, P., 2015. Particle-size segregation in dense granular avalanches. C. R. Phys. 16, 73–85.
Hajra, S.K., Khakhar, D.V., 2005. Radial mixing of granular materials in a rotating cylinder: experimental determination of particle self-diffusivity. Phys. Fluids 17, 013101 (2005).
Iverson, R.M., Costa, J.E., Lahusen, R.G., 1992. Debris-flow flume at H. J. Andrews experimental forest, Oregon. U.S. Geol. Surv. Open File Rep. 92–483 (2 pp.).
Jain, N., Ottino, J.M., Lueptow, R.M., 2005a. Combined size and density segregation and mixing in noncircular tumblers. Phys. Rev. E 71, 051301.
Jain, N., Ottino, J.M., Lueptow, R.M., 2005b. Regimes of segregation and mixing in combined size and density granular systems: an experimental study. Granul. Matter 7, 69–81.
Kadanoff, L.P., 1999. Built upon sand: Theoretical ideas inspired by granular flows. Rev. Mod. Phys. 71, 435–444.
Koenker, R., Basset, G., 1978. Regression Quantiles. Econometrica 46 (1), 33–50.
Kueppers, U., Putz, C., Spieler, O., Dingwell, D.B., 2012. Abrasion in pyroclastic density currents: insights from tumbling experiments. Phys. Chem. Earth 45-46, 33–39.
Larcher, M., Jenkins, J.T., 2013. Segregation and mixture profiles in dense, inclined flows of two types of spheres. Phys. Fluids 25, 113301.
Larcher, M., Jenkins, J.T., 2015. The evolution of segregation in dense inclined flows of binary mixtures of spheres. J. Fluid Mech. 782, 405–429.
Lee, H., Tanaka, H., 1999. Upper and lower approximation models in interval regression using regression quantile techniques. Eur. J. Oper. Res. 116, 653–666.
Lube, G., Breard, E.C.P., Cronin, S.J., Jones, J., 2015. Synthesizing large-scale pyroclastic flows: experimental design, scaling, and first results from PELE. J. Geophys. Res. Solid Earth 120, 1487–1502.
Mitani, N.K., Matuttis, H.G., Kadono, T., 2004. Density and size segregation in deposits of pyroclastic flow. Geophys. Res. Lett. 31, L15606.
Nenov, I.P., Fylstra, D.H., 2003. Interval methods for accelerated global search in the Microsoft Excel Solver. Reliab. Comput. 9 (2), 143–159.
Ottino, J.M., Khakhar, D.V., 2000. Mixing and segregation of granular materials. Annu. Rev. Fluid Mech. 32, 55–91.
Pittari, A., Cas, R.A.F., Marti, J., 2005. The occurrence and origin of prominent massive, pumice-rich ignimbrite lobes within the late Pleistocene Abrigo ignimbrite, Tenerife, Canary Islands. J. Volcanol. Geotherm. Res. 139, 271–293.
Pouliquen, O., 1999. Scaling laws in granular flows down rough inclined planes. Phys. Fluids 11, 542.
Roche, O., Gilbertson, M.A., Phillips, J.C., Sparks, R.S.J., 2004. Experimental study of gas-fluidized granular flows with implications for pyroclastic flow emplacement. J. Geophys. Res. 109, B10201. http://dx.doi.org/10.1029/2003JB002916.
Roche, O., Montserrat, S., Niño, Y., Tamburrino, A., 2010. Pore fluid pressure and internal kinematics of gravitational laboratory air-particle flows: insights into the emplacement dynamics of pyroclastic flows. J. Geophys. Res. 115, B09206. http://dx.doi.org/10.1029/2009JB007133.
Savage, S.B., Lun, C.K.K., 1988. Particle size segregation in inclined chute flow of dry cohesionless granular solids. J. Fluid Mech. 189, 311–335.
Sulpizio, R., Dellino, P., Mele, D., La Volpe, L., 2009. Generation of Pyroclastic Density Currents from Pyroclastic Fountaining or Transient Explosions: Insights from Large-Scale Experiments. IOP Conf. Series: Earth and Environmental Science 3. http://dx.doi.org/10.1088/1755-1307/3/1/012020.
Sulpizio, R., Dellino, P., Doronzo, D.M., Sarocchi, D., 2014. Pyroclastic density currents: state of the art and perspectives. J. Volcanol. Geotherm. Res. 283, 36–65.
Tripathi, A., Khakhar, D.V., 2011. Rheology of binary mixtures in the dense flow regime. Phys. Fluids 23, 113302.
Vallance, J.W., 2005. Volcanic debris flows. In: Jakob, M., Hungr, O. (Eds.), Debris-flow Hazards and Related Phenomena. Springer, Berlin Heidelberg, Praxis, pp. 247–271.
Wohletz, K.H., Sheridan, M.F., Brown, W.K., 1989. Particle size distributions and the sequential fragmentation/transport theory applied to volcanic ash. J. Geophys. Res.:94 http://dx.doi.org/10.1029/89JB01248.
Wohletz, K.H., McQueen, R.G., Morrissey, M., 1995. Experimental study of hydrovolcanism by fuelcoolant interaction analogues. Proc. NSF/JSPS AMIGO-IMI Seminar, Santa Barbara, CA, June 8–13, pp. 287–317.
Yu, K., Lu, Z., Stander, J., 2003. Quantile regression: applications and current research areas. Statisticians 52 (3), 331–350.